

Study of Atmospheric Neutrino Oscillations in SK-I and SK-II

S. Nakayama^a for the Super-Kamiokande Collaboration

(*a*) *Research Center for Cosmic Neutrinos, Institute for Cosmic Ray Research, University of Tokyo*

5-1-5 Kashiwa-no-Ha, Kashiwa-City, Chiba 277-8582 Japan

Presenter: S. Nakayama (shoei@suketto.icrr.u-tokyo.ac.jp), jap-nakayama-S-abs1-he22-oral

Using the Super-Kamiokande atmospheric neutrino data, various types of oscillation analyses are performed. For the $\nu_\mu \leftrightarrow \nu_\tau$ two flavor oscillation scenario, a zenith angle analysis with an optimum binning gives the most accurate determination of the oscillation parameters. No evidence for non-zero θ_{13} is found by a three flavor oscillation analysis with one mass scale dominance approximation.

1. $\nu_\mu \leftrightarrow \nu_\tau$ two flavor oscillation analysis (SK-I, SK-II)

The existing atmospheric neutrino data are explained very well by the pure $\nu_\mu \leftrightarrow \nu_\tau$ two flavor oscillation scheme [1, 2]. To get a better constraint on the oscillation parameters, a zenith angle analysis with an optimum binning is performed using the Super-Kamiokande-I atmospheric neutrino data from a 1489 day exposure. In the analysis, fully-contained (FC), partially-contained (PC), and upward-going muon events are divided in 37 momentum and event type bins: 5 (5) for the FC single-ring sub-GeV e -like (μ -like) sample, 5 (3) for the FC single-ring multi-GeV e -like (μ -like) sample, 5 (4) for the FC multi-ring e -like (μ -like) sample, 4 (4) for the PC stopping (through-going) sample, and 1 (1) for the upward stopping (through-going) muon sample. All samples are divided in 10 zenith angle bins. The number of observed events in each of 370 bins is compared with the Monte Carlo expectation by the $\nu_\mu \leftrightarrow \nu_\tau$ two flavor oscillation scenario. A χ^2 statistic is defined assuming the Poisson distribution. During the fit, the expected number of events in each bin is recalculated to account for systematic variations due to uncertainties in the neutrino flux model, neutrino cross-section model, and detector response. A global scan is made on a $(\sin^2 2\theta, \log \Delta m^2)$ grid minimizing χ^2 at each point with respect to 45 systematic error parameters. Among the 45 parameters, 39 parameters are common to the previous

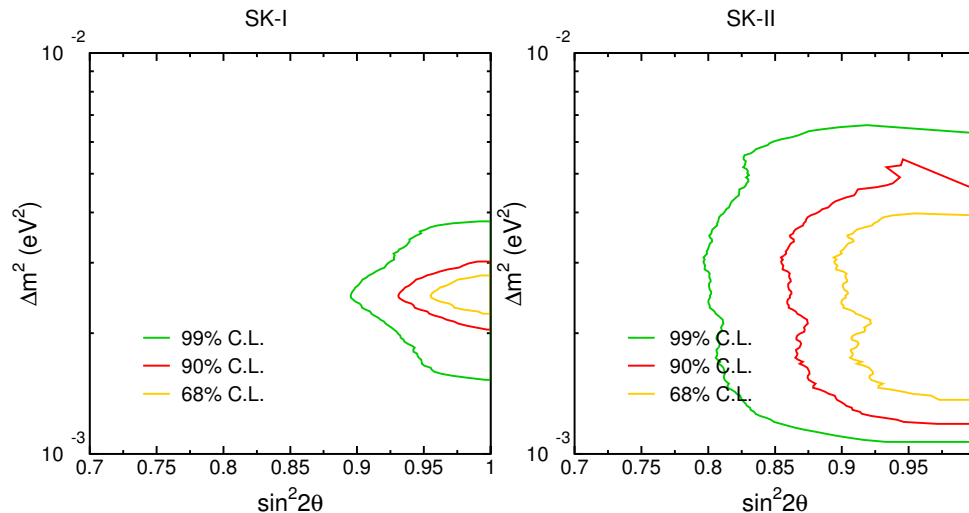


Figure 1. Allowed oscillation parameters for $\nu_\mu \leftrightarrow \nu_\tau$ oscillations by the SK-I data (left) and the SK-II data (right).

analysis described in Ref. [1]. The other parameters are for uncertainties on background subtraction from the upward through-going muon sample, background subtraction from the upward stopping muon sample, non- ν_e contamination in the multi-GeV single-ring e -like sample, non- ν_e contamination in the multi-GeV multi-ring e -like sample, normalization of the multi-GeV single-ring e -like sample, and relative normalization between the PC stopping and PC through-going samples. The minimum χ^2 value in the physical region, $\chi_{\min}^2 = 375.2/368$ DOF, is located at ($\sin^2 2\theta = 1.00$, $\Delta m^2 = 2.5 \times 10^{-3} \text{ eV}^2$). Figure 1 (left-hand) shows contours of allowed oscillation parameter regions corresponding to the 68 %, 90 % and 99 % confidence intervals. The measured parameters are $\sin^2 2\theta > 0.93$ and $2.0 \times 10^{-3} < \Delta m^2 < 3.2 \times 10^{-3} \text{ eV}^2$ at 90 % confidence level.

The same analysis is carried out using the Super-Kamiokande-II atmospheric neutrino data from a 627 day exposure. Super-Kamiokande-II started physics measurements in January 2003 with about a half of the original PMT density in the inner detector. Each inner detector PMT is enclosed by an acrylic vessel to prevent chain implosions. In the analysis, most of the systematic errors related to the detector response are re-evaluated for the SK-II data. The minimum χ^2 value, $\chi_{\min}^2 = 394.5/368$ DOF, is located at ($\sin^2 2\theta = 0.98$, $\Delta m^2 = 3.1 \times 10^{-3} \text{ eV}^2$). The allowed oscillation parameter region is shown in Figure 1 (right-hand). The oscillation parameters are measured to be $\sin^2 2\theta > 0.85$ and $1.2 \times 10^{-3} < \Delta m^2 < 5.5 \times 10^{-3} \text{ eV}^2$ at 90 % confidence level. The result is consistent with measurement by the SK-I data.

2. Three flavor oscillation analysis (SK-I)

There is no evidence for the oscillation of atmospheric ν_e at present. As for the 1–3 mixing parameter, only the upper limit of $\sin^2 \theta_{13}$ has been obtained by the CHOOZ reactor neutrino experiment [3]. To search for an evidence of non-zero θ_{13} , the SK-I atmospheric neutrino data are analyzed in the three flavor neutrino oscillation scheme with the one mass scale dominance approximation ($\Delta m_{12}^2 \sim 0$, $\Delta m_{13}^2 \sim \Delta m_{23}^2 \equiv \Delta m^2$). In this scenario, oscillation probabilities can be expressed with three parameters, $\sin^2 \theta_{13}$, $\sin^2 \theta_{23}$ and Δm^2 [4, 5]. In case of the normal mass hierarchy (i.e., $\Delta m^2 > 0$), the oscillation probability involving electron neutrinos is enhanced by the Earth's matter effect [6, 7] resonantly for neutrino energy around 3~10 GeV, while

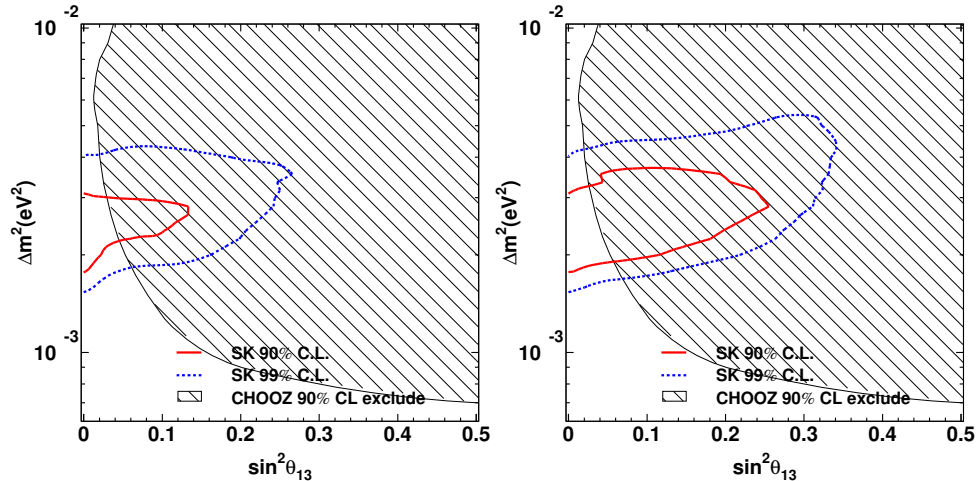


Figure 2. Allowed oscillation parameters by a three flavor oscillation analysis with the SK-I data in case of the normal mass hierarchy (left) and the inverse mass hierarchy (right). The excluded region by CHOOZ is also shown.

there is no resonance in the oscillation probability for electron anti-neutrinos. On the other hand, in case of the inverse mass hierarchy (i.e., $\Delta m^2 < 0$), the oscillation probability concerned with electron anti-neutrinos is enhanced and no resonance is seen for electron neutrinos. The oscillation probability is calculated with an approximation about the Earth's matter density as follows: $\rho = 13.0 \text{ g/cm}^3$ in $R=0-1221 \text{ km}$, 11.3 g/cm^3 in $R = 1221-3480 \text{ km}$, 5.0 g/cm^3 in $R = 3480-5701 \text{ km}$, and 3.3 g/cm^3 in $R = 5701-6371 \text{ km}$, where R represents distance from the Earth center. The data set and its binning, the definition of χ^2 and its minimization at each oscillation parameter point, and the systematic errors are the same as those of the two flavor analysis described in this paper. Figure 2 (left-hand) shows contours of allowed oscillation parameter regions corresponding to the 90% and 99% confidence intervals in case of the normal mass hierarchy. The minimum χ^2 value, $\chi_{\min}^2 = 376.82/368 \text{ DOF}$, is located at ($\sin^2 \theta_{13} = 0.0$, $\sin^2 \theta_{23} = 0.5$, $\Delta m^2 = 2.5 \times 10^{-3} \text{ eV}^2$). The result is consistent with the pure $\nu_\mu \leftrightarrow \nu_\tau$ two flavor oscillation hypothesis. The allowed region in case of the inverse mass hierarchy is also shown in Figure 2 (right-hand). The minimum χ^2 value, $\chi_{\min}^2 = 376.76/368 \text{ DOF}$, is located at ($\sin^2 \theta_{13} = 0.00625$, $\sin^2 \theta_{23} = 0.525$, $\Delta m^2 = 2.5 \times 10^{-3} \text{ eV}^2$). It is found that the SK-I data show no evidence for non-zero θ_{13} in both the normal and inverse mass hierarchy scenarios.

3. Oscillation analysis including the solar neutrino oscillation parameters (SK-I)

Recently, the 1–2 oscillation parameters were measured with the great precision by combining solar neutrino data [8, 9] and the KamLAND reactor neutrino data [10]. If these LMA-MSW oscillation parameters are taken into consideration, the oscillation of low energy (below 1 GeV) atmospheric ν_e 's is expected to appear at some level regardless with the existence of the non-zero θ_{13} . We assume $\theta_{13} = 0$ for the analysis in this section. As widely discussed in the literature [11, 12], the relative change on the atmospheric ν_e flux due to oscillations driven by the solar neutrino parameters is written as follows: $F_e^{\text{osc}}/F_e^0 - 1 = P_2 (r \cos^2 \theta_{23} - 1)$, where F_e^{osc} and F_e^0 are the atmospheric ν_e fluxes with and without oscillations, and $r \equiv F_\mu^0/F_e^0$ is the ratio of the original atmospheric ν_μ and ν_e fluxes. P_2 is the two neutrino transition ($\nu_e \rightarrow \nu_x$) probability in matter driven by the 1–2 parameters. The factor in brackets in the equation is called the ‘‘screening’’ factor. In fact, since the ν_μ and ν_e flux ratio $r \sim 2$ in the sub-GeV neutrino energy region [13, 14, 15], the screening factor is very small in the case of the maximal 2–3 mixing (i.e., $\theta_{23} = 45^\circ$). If θ_{23} is in the first octant, $\theta_{23} < 45^\circ$, the screening factor is positive and an excess of the sub-GeV e -like sample is expected. If θ_{23} is in the second octant, $\theta_{23} > 45^\circ$, the screening factor is negative and the sub-GeV e -like sample is expected to be reduced. Thus, an oscillation analysis of the sub-GeV samples taking into account the sub-dominant 1–2 oscillation has the possibility to determine the octant of θ_{23} for the non-maximal $\sin^2 2\theta_{23}$. Of course, the deviation of $\sin^2 2\theta_{23}$ affects other observables, especially the zenith angle dependence of μ -like events. Therefore in order to determine $\sin^2 \theta_{23}$, we need a combined oscillation analysis of all the samples with systematic errors properly estimated.

Since $\theta_{13} = 0$ is assumed in this analysis as previously mentioned, χ^2 is calculated in the four dimensional oscillation parameter space of Δm_{12}^2 , Δm_{23}^2 , $\sin^2 \theta_{12}$ and $\sin^2 \theta_{23}$. For the solar neutrino parameters, we examine two scenarios. In the scenario with the solar neutrino parameters turned on, the solar neutrino parameters are chosen around the allowed region obtained by a combined analysis of the solar neutrino data and KamLAND data. To give a constraint on the solar neutrino parameters, the χ^2 value by the combined analysis of the solar neutrino and KamLAND data is added to χ^2 from the SK-I atmospheric neutrino data for each (Δm_{12}^2 , $\sin^2 \theta_{12}$) point. The other scenario is ordinary ‘‘one mass scale dominance’’ approximation with $\Delta m_{12}^2 = 0$, that is, pure $\nu_\mu \leftrightarrow \nu_\tau$ two flavor oscillation scenario. The data set and its binning, the definition of χ^2 and its minimization at each oscillation parameter point, and the systematic errors are the same as those of the two flavor zenith angle analysis described in this paper. Figure 3 shows the $\sin^2 \theta_{23}$ dependence of the $\chi^2 - \chi_{\min}^2$ function marginalized with respect to Δm_{12}^2 , Δm_{23}^2 and $\sin^2 \theta_{12}$, for two scenarios with and without the solar neutrino parameters. It is found that the best-fit point is located around $\sin^2 \theta_{23} = 0.5$ in both cases.

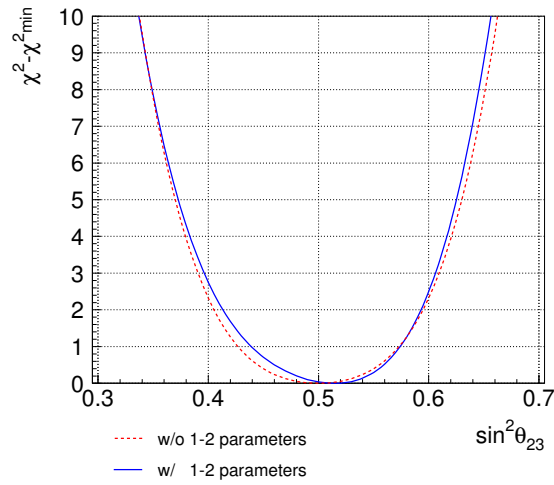


Figure 3. The $\chi^2 - \chi_{\min}^2$ distribution as a function of $\sin^2 \theta_{23}$ for oscillations without the 1–2 parameters (red dashed line) and with the 1–2 parameters (blue solid line) by the SK-I atmospheric neutrino data. $\theta_{13} = 0$ is assumed. For each $\sin^2 \theta_{23}$ point, the other oscillation parameters are chosen to minimize χ^2 .

4. Conclusion

In the $\nu_\mu \leftrightarrow \nu_\tau$ two flavor oscillation scheme, the zenith angle analysis with an optimum binning gives the most accurate determination of the oscillation parameters using the SK-I data, $\sin^2 2\theta > 0.93$ and $2.0 \times 10^{-3} < \Delta m^2 < 3.2 \times 10^{-3} \text{ eV}^2$ at 90% confidence level. The zenith angle analysis using the SK-II data gives the consistent result. In the three flavor oscillation analysis with one mass scale dominance approximation, no evidence for non-zero θ_{13} is observed in the SK-I data. An oscillation analysis taking into account the solar neutrino parameters gives no significant change on the result by the analysis without the solar parameters.

References

- [1] Y. Ashie *et al.* [Super-Kamiokande Collaboration], arXiv:hep-ex/0501064.
- [2] Y. Ashie *et al.* [Super-Kamiokande Collaboration], Phys. Rev. Lett. **93**, 101801 (2004)
- [3] M. Apollonio *et al.*, Eur. Phys. J. C **27**, 331 (2003)
- [4] G. L. Fogli, E. Lisi, D. Montanino and G. Scioscia, Phys. Rev. D **55**, 4385 (1997)
- [5] C. Giunti, C. W. Kim and M. Monteno, Nucl. Phys. B **521**, 3 (1998)
- [6] L. Wolfenstein, Phys. Rev. D **17**, 2369 (1978).
- [7] S. P. Mikheev and A. Y. Smirnov, Sov. J. Nucl. Phys. **42**, 913 (1985) [Yad. Fiz. **42**, 1441 (1985)].
- [8] S. N. Ahmed *et al.* [SNO Collaboration], Phys. Rev. Lett. **92**, 181301 (2004)
- [9] M. Smy *et al.* [Super-Kamiokande Collaboration], 29th ICRC, Pune (2005).
- [10] T. Araki *et al.* [KamLAND Collaboration], Phys. Rev. Lett. **94**, 081801 (2005)
- [11] O. L. G. Peres and A. Y. Smirnov, Phys. Lett. B **456**, 204 (1999)
- [12] O. L. G. Peres and A. Y. Smirnov, Nucl. Phys. B **680**, 479 (2004)
- [13] M. Honda, T. Kajita, K. Kasahara and S. Midorikawa, Phys. Rev. D **70**, 043008 (2004)
- [14] G. D. Barr, T. K. Gaisser, P. Lipari, S. Robbins and T. Stanev, Phys. Rev. D **70**, 023006 (2004)
- [15] G. Battistoni, A. Ferrari, T. Montaruli and P. R. Sala, arXiv:hep-ph/0305208.